J Mater Sci (2007) 42:2678–2683
DOI 10.1007/s10853-006-1367-y

Effect of the oxygen pressure on the photoluminescence properties of ZnO thin films by PLD

X. M. Fan · J. S. Lian · Qing Jiang · ZuoWan Zhou

Received: 12 July 2005 / Accepted: 22 February 2006 / Published online: 4 January 2007
© Springer Science+Business Media, LLC 2007

Abstract ZnO thin films on Si(111) substrate were deposited by laser ablation of Zn target in oxygen reactive atmosphere; Nd-YAG laser with wavelength of 1064 nm was used as laser source. The experiments were performed at laser energy density of 31 J/cm^2, substrate temperature of 400 °C and various oxygen pressures (5–65 Pa). X-ray diffraction was applied to characterize the structure of the deposited ZnO films and the optical properties of the ZnO thin films were characterized by photoluminescence with an Ar ion laser as a light source using an excitation wavelength of 325 nm. The influence of the oxygen pressure on the structural and optical properties of ZnO thin films was investigated. It was found that ZnO film with random growth grains can be obtained under the condition of oxygen pressure 5–65 Pa. It will be clearly shown that the grain size and the formation of intrinsic defects depend on the oxygen partial pressure and that high optical quality of the ZnO films is obtained under low oxygen pressure (5 Pa, 11 Pa) conditions.

X. M. Fan · Z. W. Zhou
College of Materials Engineering, Southwest Jiaotong University, Chengdu, Sichuan 610031, China

X. M. Fan (✉) · J. S. Lian · Q. Jiang
Key Lab of Automobile Materials, Ministry of Education, College of Materials Science and Engineering, Jilin University, Changchun 130025, China
e-mail: fanximei@126.com

Introduction

One important advantage of ZnO is that it is a II–VI semiconductor of wurtzite structure with a wide direct-band-gap of 3.2 eV [1] at room temperature. Wide and direct band gap semiconductors are of interest for blue and ultra-violet optical devices, such as light-emitting diodes and laser diodes [2–4]. The other notable advantage of ZnO is its high exciton binding energy (60 meV) at room temperature, which in principle allows efficient excitonic lasing mechanism operating at RT. It was reported that the corresponding photoluminescence spectra of ZnO films show defect-related deep-level emissions as well as ultraviolet (UV) near-band-edge emission around 380 nm [5]. The UV-emission properties of ZnO films depend critically on their microstructure. Excellent UV emission quality can be obtained from ZnO films with high *c*-axis-oriented structure [6]. High intensity emission from ZnO films have been deposited by using several growth techniques, such as metal-organic chemical vapour deposition (MOCVD) [7], molecular beam epitaxy (MBE) [8], sol–gel deposition [9], rf magnetron sputtering [10] and reactive DC sputtering [11, 12], oxidation of metal zinc film [13], pulsed laser deposition (PLD) [14]. Pulsed laser deposition (PLD) technique is more useful in obtaining high quality thin films of metal oxide materials compared with other techniques, because of its advantage of simple hardware, atomic-layer control obtained by adjusting the laser energy density, the pulse duration and repetition rate. The plasma fabricated by the pulsed laser ablation is very energetic and its mobility can be easily controlled by changing the processing parameter. For these practical reasons,

PLD technique has been widely applied for the formation of the high quality thin films.

The excimer laser (pulse duration of 10 ns) and high purity ZnO target (99.99% purity) have been widely used to grow ZnO thin films during the process of PLD [15–17]. However, few reports were published on long wavelength Laser (wavelength of 1064 nm, pulse duration of 100 ns) and Zn target (99.99% purity) applied in the growth of ZnO by PLD. In consideration of low-cost preparation of ZnO film, in the present work, we applied a very common Laser apparatus (Nd-YAG laser of 1064 nm) and a Zn target (which is much cheaper than ZnO target) to deposit ZnO thin films under oxygen pressure. The structural and optical properties of ZnO thin films obtained at different oxygen pressure are investigated. XRD and PL were used to characterize the effect of the oxygen pressure on the structural and optical properties of ZnO thin films.

Experimental

Si(111) substrate was used as the underlay and it was carefully cleaned prior to the deposition. The experiments were performed in a vacuum chamber. After the sample was loaded into chamber, the vacuum chamber was evacuated by turbo-molecular pump down to 5×10^{-4}Pa and then filled with oxygen (99.99% purity). The laser energy density was measured to be about 31 J/cm^2, Zn (99.99% purity) targets were ablated by a Nd-YAG laser (wavelength of 1064 nm, pulse duration of 100 ns, frenquency of 10 Hz). The ZnO films were deposited at the substrate temperature of 400 °C and various oxygen pressures (5–65 Pa) .The target–substrate distance was kept at 2.5 cm. The deposition time of 20 min was maintained. The film thickness measured by the cross section image of SEM was about 0.6–1.0 μm, which depends on the oxygen pressures. After deposition, ZnO film was cooled from 400 °C to room temperature with the corresponding growth ambient in the deposition chamber. ZnO film crystal structure was investigated by X-ray diffraction (XRD, Rigaku Dymax) with a Cu target and a monochronmator at 50 kV and 300 mA. The optical properties of the ZnO thin films were characterized by photoluminescence with an Ar ion laser as a light source using an excitation wavelength of 325 nm. All spectra were measured at room temperature.

Results and discussion

Figure 1 shows the XRD of the ZnO thin films on Si(111) substrate obtained by laser ablation of Zn target in oxygen reactive atmosphere at the substrate temperature of 400 °C and various oxygen pressures (5–65 Pa). Five diffraction peaks of ZnO thin films appear at 2θ = 31.81°, 34.46°, 36.27°, 47.67° and 56.79°, which are corresponding to the (100), (002), (101), (102) and (110) planes of ZnO thin films, respectively. It is seen that the films obtained at various oxygen pressure (5–65 Pa) have random polycrystalline structure without clearly preferred orientation. With the increase of oxygen pressure, the diffraction peaks become more intense and sharper, which suggests that the grain size becomes larger and the crystal quality has improved. In order to evaluate the average grain size of the films, we adopted the Scherrer formula using the full width at half maximum (FWHM) value of the XRD diffraction peaks. The Scherrer formula is $d = 0.94\lambda/B \cos \theta$, where d, λ, θ, and B are the mean grain size, the X-ray wavelength of 0.154 Å, Bragg diffraction angle, and the FWHM of the diffraction peak of ZnO film (101) direction at 36.27°, respectively. The mean grain sizes are 16.5, 17.9, 18.6, 26.45 and 26.7 nm for the ZnO films deposited at oxygen pressure of 5, 11, 30, 40 and 65 Pa, respectively. This result indicates that the grain size increases with increasing oxygen pressure. It should be emphasized that the broadening of the peaks occurs for two reasons: (i) limitations in the spatial extent of the coherent scattering volume (in our case the grain size), and (ii) the presence of inhomogeneous strain (for example dislocations) [18]. Therefore, the FWHM of peaks measured by XRD should include other growth defects, for example, lattice or extrinsic GB (grain boundary) dislocations, which are often formed in nanocrystalline structures. The micrographs of atomic force microscopy (AFM) of the samples grown at the oxygen pressure of 11, 30 and 65 Pa were shown in

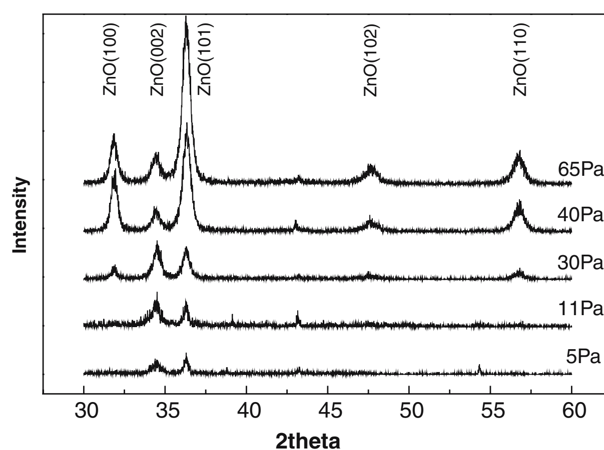

Fig. 1 The XRD of ZnO films obtained at 400 °C with different oxygen pressure

Fig. 2. It is seen from Fig. 2 that the ZnO films are composed of the polycrystalline structure with inhomogeneous and random orientation grains, and the grain sizes slightly increase with the increasing oxygen pressure. Also, the rougher surface from ZnO films is formed with the increasing oxygen pressure (for example, RMS from ZnO films is 51.7, 51.8 and 68.2 nm at the oxygen pressures of 11, 30 and 65 Pa, respectively). This consists well with the above XRD analysis results.

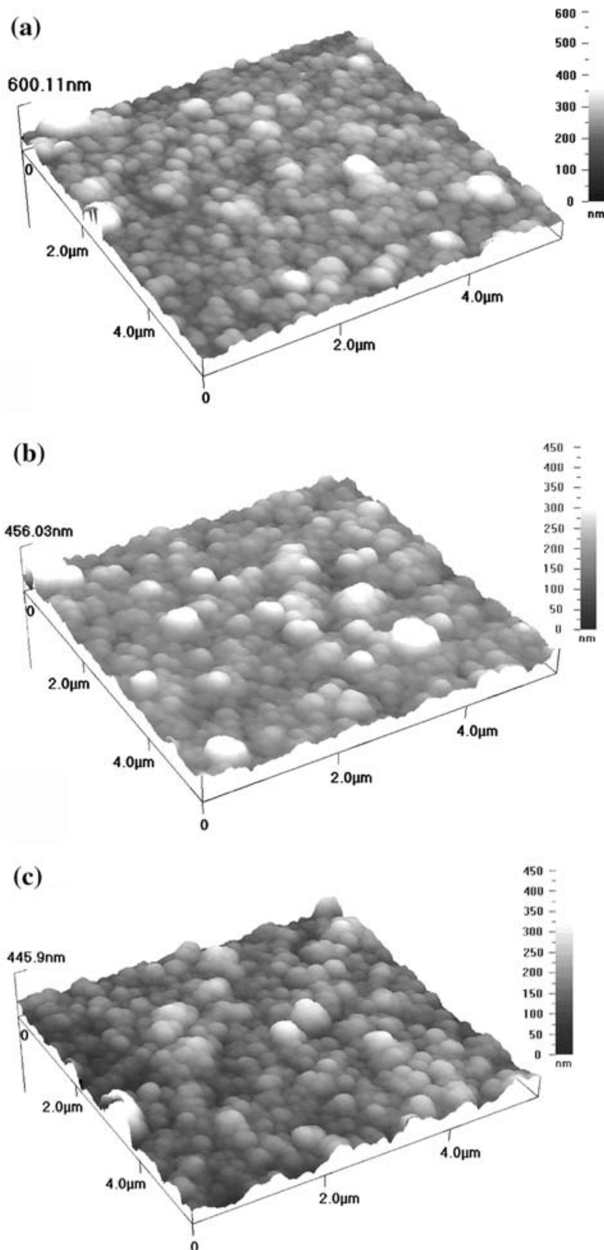

Fig. 2 AFM images of ZnO thin films obtained at 400 °C with the oxygen pressure (**a**) 11 Pa, (**b**) 30 Pa and (**c**) 65 Pa, respectively

Figure 3 shows room temperature photoluminescence (PL) spectra of ZnO films on silicon substrate. All the spectra are dominated by strong UV emission centering at 373–383 nm and wide green emission centering at 518–535 nm. It can be seen from Fig. 3 that the peak intensity and peak position of UV emission vary with the oxygen pressure. The intensity and position of the UV emission peak are replotted as a function of the oxygen pressure in Fig. 4. It is found from Fig. 4 that the intensity of UV emission is the largest in the sample deposited at oxygen pressure of 40 Pa, and the lowest in the sample deposited at oxygen pressure of 11 Pa. The UV emission peaks of the samples deposited at 5–11 Pa center around 373 nm (or 3.31 eV), while those of the samples deposited at 30–65 Pa center around 383 nm (or 3.23 eV). Generally, the room temperature UV emission is thought to originate from free excitonic emission because of the high exciton binding energy of 60 meV [19], the typical peak position reported is at 3.26 eV (or 379 nm) [20]. Therefore, it can be seen that the UV peak position shifts towards longer wavelength at higher oxygen pressures (30 Pa, 40 Pa, 65 Pa), while the UV peak position shifts towards shorter wavelength at lower oxygen pressures (5 Pa, 11 Pa). The energy shift of UV emission of the sample deposited at the different pressure (5–65 Pa) is about 80 meV. The energy shift of the UV emission peak of ZnO films with nanometer scale grain size may be attributed to the energy gap enhancement due to the quantum confinement effect. According to quantum confinement theory, the energy band gap of a semiconductor depends on the crystal size. An expression [21] for the energy gap, including the quantum confinement effect, is

$$E_g \approx E_{g_0} + h^2\pi^2\mu/2d^2 - 1.8e^2/\varepsilon d$$

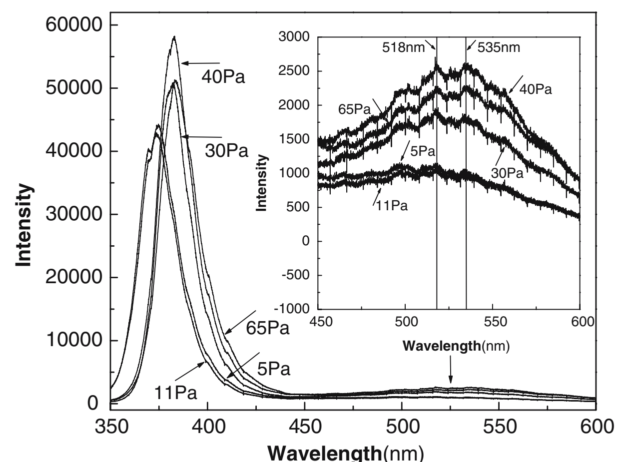

Fig. 3 PL spectra of ZnO films at 400 °C with different oxygen pressures

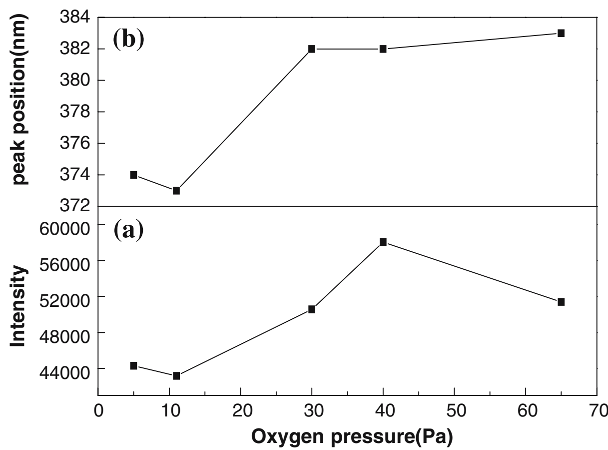

Fig. 4 The intensity and peak position of UV emission of PL spectra of ZnO films obtained at different oxygen pressures

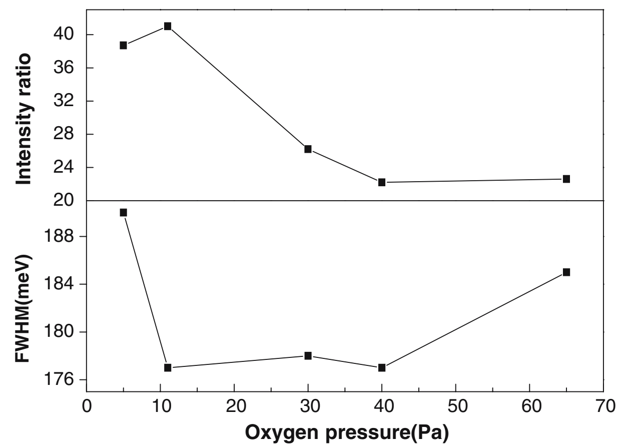

Fig. 5 The FWHM of UV emission and the ratio of UV intensity to deep level emission of PL spectra of ZnO films obtained at different oxygen pressures

where E_{g_0} is the energy gap for bulk materials, d is the grain size, $1/\mu = 1/m_e + 1/m_h$ (m_e and m_h being the electron and hole effective masses, respectively), and ε is the dielectric constant. For ZnO film, $m_e = 0.38m_0$, $m_h = 1.80m_0$ and $\varepsilon = 8.75$ [22]. The above XRD analysis results show the average grain size in the ZnO films increases from 16.5 to 26.7 nm with an increase of oxygen pressure from 5 to 65 Pa. Introducing these experimental data into the equation, the calculated enhancement of band gap due to the quantum confinement effect is about 128 meV. It is reasonable that the enhancement of band gap theoretically calculated is somewhat larger than the energy shift (80 meV) of UV emission obtained experimentally, as the energy shift is restricted by the enhancement of band gap. Similar energy gap enhancement in nanocrystalline ZnO was also reported [23, 24].

In order to evaluate photoluminescence quality of ZnO films, FWHM of the UV emission peak and the intensity ratio of UV emission to deep level emission are plotted as a function of the oxygen pressure in Fig. 5. It is found that the FWHM value of the UV emission peak obtained from the films grown at different oxygen pressure varies only in a narrow range (177–190 meV), while the intensity ratio of the UV emission to the deep level emission decreases as oxygen pressure increases. A maximum intensity ratio value 41 was observed from the film grown at oxygen pressure 11 Pa. The obtained intensity ratio is similar to the value obtained by annealing ZnO nanocrystals embedded in CaF_2 matrix at 700 °C [25]. And the FWHM values are comparative to that value (187 meV) reported for the ZnO films obtained by PLD with eximer Laser [26]. It is well known that small FWHM of the UV emission peak and high intensity ratio of UV emission to deep level emission represent good optical quality for ZnO films. Therefore, the above results indicate that ZnO film deposited by laser ablation of Zn target in oxygen reactive atmosphere at the substrate temperature of 400 °C and oxygen pressure of 11 Pa has a good optical quality.

It can be seen from Fig. 3 that the intensity of green emission peaks is relative larger at high oxygen pressure (30–65 Pa), while that is small at low oxygen pressure (5–11 Pa). The origins of the green emission of ZnO film have been investigated, however, due to the complexity of the microstructure of ZnO, there is still no satisfactory consensus. Vanheusden et al. [27] has found a strong correlation between the green emission and singly ionized oxygen vacancies. They thought that the ionized oxygen vacancies were responsible for the green emission. Zhang et al. [28] reported that the green emission may originate from the electron transition from the level of the ionized oxygen vacancies to the valence band. Lin et al. [29] thought that green emission corresponds to the electron transition from the bottom of the conduction band to the antisite defect O_{Zn} level.

It is well known that there are five intrinsic defects in ZnO film, such as zinc vacancy V_{Zn}, oxygen vacancy V_O, interstitial zinc Zn_i, interstitial oxygen O_i, and antisite oxygen O_{Zn} [29, 30]. During deposition, the variation of these defects with the oxygen pressure (P_{O_2}) can be expressed as the following [28]:

$$\frac{1}{2}O_2 + V_O^x = O_O^x, \ldots [V_O^x] \propto P_{O_2}^{-1/2} \quad (1)$$

$$\frac{1}{2}O_2 = V_{Zn}^x = O_O^x, \ldots[V_{Zn}^x] \propto P_{O_2}^{1/2} \quad (2)$$

$$Zn_i + \frac{1}{2}O_{2(g)} = Zn_{Zn} + O_o, \ldots[Zn_i] \propto P_{O_2}^{-1/2} \quad (3)$$

$$\frac{1}{2}O_2 = O_i, \ldots[O_i] \propto P_{O_2}^{1/2} \quad (4)$$

$$\frac{1}{2}O_{2(g)} + V_{Zn} = O_{Zn}, \ldots[O_{Zn}] \propto P_{O_2}^{1/2}[V_{Zn}] \quad (5)$$

Here, $[V_O^x]$ and $[V_{Zn}^x]$ are the concentrations of the nonionized vacancies of oxygen and zinc, respectively. $[Zn_i]$, $[O_i]$, and $[O_{Zn}]$ are the concentrations of the interstitial zinc Zn_i, interstitial oxygen O_i and antisite oxygen O_{Zn}, respectively. Therefore, Eqs. 1 and 3 indicate that the concentrations of the V_O and the Zn_i decrease with the increase of the oxygen pressure. Eqs. 2, 4 and 5 indicate that the concentrations of the zinc vacancy V_{Zn}, the interstitial oxygen O_i and the antisite oxygen O_{Zn} increase with the increase of the oxygen pressure P_{O_2}. The present experimental results showed that relatively strong deep level emission occurred from the ZnO films grown at high oxygen pressure (see Fig. 3). Therefore, it can be deduced that the origins of the green emission of ZnO film may be concerned with the zinc vacancy V_{Zn}, the interstitial oxygen O_i and the antisite oxygen O_{Zn}. Sun's calculated results [31] were cited to confirm that which defects on earth were related with the origins of the green emission of ZnO film. Sun calculated the energy levels of the intrinsic defects in ZnO films by using the full-potential linear muffin orbital method (see Fig. 6). It is seen from Fig. 6 that the calculated energy interval from the bottom of the conduction band to the three defect levels are 2.38 eV to O_{Zn}, 2.28 eV to O_i and 3.06 eV to V_{Zn}, respectively. It is seen from Fig. 3 that the green emissions of PL spectra of ZnO films grown at relatively high oxygen pressure had two jointed peaks centering at 518 and 535 nm, respectively, which corresponds to the energy levels of 2.386 and 2.310 eV, respectively. Therefore, it can be deduced that the electron transition from the bottom of the conduction band to the antisite oxygen O_{Zn} defect levels should be main origins corresponding to the green emission of PL spectra in our experiment. Also, the O_i defects are another possible origins for the green emission, as one of the experimental energy peak positions (2.31 eV) is approximately consistent with the calculated O_i defect's level (2.28 eV).

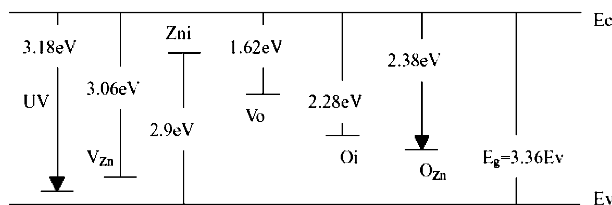

Fig. 6 The draft of calculated defect's levels in ZnO film (Ref. [31])

Conclusion

ZnO thin films with random orientation on Si(111) substrate were formed by the laser ablation of Zn target in oxygen atmosphere with a Nd-YAG laser of 1064 nm wavelength as the pulse laser source and at the substrate temperature 400 °C. The influences of oxygen pressure on the optical properties of ZnO film were studied. It was found that all films grown at different oxygen pressure ranging from 5 to 65 Pa show typical luminescence behavior, but the films formed at low oxygen pressure (for example, 11 Pa) exhibit a high intensity ratio (41) of UV emission to deep level emission and a slightly narrow FWHM of UV emission. The UV peak shifts from 3.23 to 3.31 eV as oxygen pressure decreases can be explained by the structure variation, which could be attributed to the gap enhancement due to the quantum confinement effect. As to the green emission, the two jointed peaks centering at 518 nm (2.386 eV) and 535 nm (2.310 eV) indicate that the electron transitions from the bottom of the conduction band to the antisite oxygen O_{Zn} and the interstitial oxygen O_i defect levels should mainly contribute to the green emission of PL spectra.

Acknowledgements This work was supported by Foundation of National Key Basic Research and Development Program (No. 2004CB619301) and Project 985-automotive engineering of Jilin University.

References

1. Berger LI (1997) Semiconductor materials. CRC Press, New York
2. Zu P, Tang ZK, Wong GKL, Kawasaki M, Ohtomo A, Koinuma H, Segawa Y (1997) Solid State Commun 103(8):459
3. Hayamizu S, Tabata H, Tanaka H, Kawai T (1996) J Appl Phys 80(12):787
4. Sun XW, Kwok HS (1999) J Appl Phys 86(12):408

5. Bethke S, Pan H, Wesseis BW (1988) Appl Phys Lett 52:138
6. Fan XM, Lian JS, Guo ZX, Lu HJ (2005) Appl Surf Sci 239:176
7. Park WI, Yi GC (2001) J Electron Mater 30(12):L32
8. Ko HJ, Chen YF, Zhu Z, Yao T, Kobayashi I, Uchiki H (2000) Appl Phys Lett 76(26):1905
9. Natsume Y, Sakata H (2000) Thin Solid Films, 372(1):30
10. Kim KK, Song JH, Jung HJ, Choi WK, Park SJ, Song JH (2000) J Appl Phys 87(12):3573
11. Zhang GB, Shi CS, Han ZF, Shi JY, Fu ZX, Kirm M, Zimmerer G (2001) Chin Phys Lett 18(3):441
12. Guo CX, Fu ZX, Shi CS (1999) Chin Phys Lett 16(9):146
13. Chen XJ, Liu YC, Ma JG (2002) J Crystal Growth 240(3–4):467
14. Jin BJ, Im S, Lee SY (2000) Thin Solid Films 366(1–2):107
15. Ryu YR, Zhu S, Wrobel JM (2000) J Crystal Growth 216(1–4):326
16. Hu WS, Liu ZG, Sun J, Zhu SN, Xu QQ, Feng D, Ji ZM (1997) J Phys Chem Solids 56(6):849
17. Craciun V, Amirhaghi S, Craciun D (1995) Appl Surf Sci 86(1–4):99
18. Budrovic Z, Van Swygenhoven H, Derlet PM, Van Petegem S, Schmitt B (2004) Science 304:273
19. Chen Y, Bagnall DM, Koh Hj, Park KT, Hiraga K, Zhu ZQ, Yao T (1998) J Appl Phys 84(12):3912
20. Bagnall DM, Chen YF, Shen MY, Zhu Z, Goto T, Yao T (1998) J Crystal Growth 184/185:605
21. Brus LE (1984) J Chem Phys 80(12):4403
22. Cho S, Ma J, Kim Y, Sun Y, George K, Wong L, Ketterson JB (1999) Appl Phys Lett 75(26):2761
23. Srikant V, Clarke DR (1997) J Mater Res 12:1425
24. Zhao D, Pan X (1994) J Vac Sci Technol B 12(5):2880
25. Liu YC, Xu HY, Mu R, Henderson DO (2003) Appl Phys Lett 83(26):1210
26. Nakata Y, Budi Hartanto A, Kawakami M, Okada T, (2003) Proc SPIE 4830:238
27. Vanheusden K, Warren WL, Seage CH, Tallent DR, Voigtang JA, Gnade BE (1996) J Appl Phys 79(12):7983
28. Zhang DH, Xue ZY, Wang QP, Ma J (2004) Proc SPIE 4918:425
29. Lin B, Fu Z, Jia Y (2001) Appl Phys Lett 79(27):943
30. Bylander EG (1978) J Appl Phys 49(12):1188
31. Sun YM (2000) Ph.D. thesis, University of Science and Technology of China